Institut für Pharmazie, Fachbereich Chemie und Pharmazie der Johannes-Gutenberg-Universität, Mainz, Germany

Functionalized and [*a*]-anellated carbazoles as potential B-DNA ligands: Experimental studies of DNA binding and molecular modeling of intercalation complexes

U. Pindur, A. Marotto, E. Schulze and G. Fischer

Three synthetically available carbazole derivatives **3**–**5** were investigated for DNA binding (ethidium bromide displacement assay, DNA unwinding assay), for inhibition of topoisomerase I and for cell cytotoxicity (antitumour cell lines). In addition molecular modeling studies of DNA complexes were performed by semiempirical quantum chemistry, force field calculations and molecular dynamics calculations. In summary, combining the results from experiments and molecular modeling, the naphthoquinone anellated carbazole **4** emerges as a promising antitumour active candidate for further drug design studies in carbazole chemistry.

1. Introduction

Anellated indoles and anellated carbazoles are pharmacologically interesting compounds of potential value as leads for the development of antitumour active drugs [1–5]. In this context, derivatives of the pyrido[4,3-*b*]carbazole alkaloid ellipticine (**1**) which intercalates into DNA and inhibits topoisomerase II are used clinically to inhibit the growth of several human tumours [1, 6–8]. In close structural relationship to the antitumour and DNA intercalator drugs of the anthracycline series as well as in close structural relationship to the intercalating drug mitoxantrone (**2**), we have synthesized a variety of new anellated indoles and anellated carbazoles [9–15]. From this series of products, the 1,2-dimethoxycarbonyl carbazole **3**, the naphthoquinone anellated carbazole **4** and the pyrrolo[*a*]anellated carbazole **5** have prompted our interest during the search for new antitumour active lead compounds in the carbazole series, which interact with the B-DNA [6].

In the present paper, in which we continue our studies of DNA ligands as potential anticancer drugs, we report the tumour cell cytotoxicity towards three different human tumour cell lines and the DNA binding characteristics of the carbazoles **3**–**5** [15, 19]. The DNA binding properties were studied employing the ethidium displacement assay, the unwinding assay and the topoisomerase I inhibition assay [7, 20–25]. In addition, in order to rationalize the experimental findings, computer molecular modeling studies were performed with appropriate B-DNA oligomers on the basis of molecular mechanics and molecular dynamics calculations and interaction field analysis [19, 26–27]. Moreover, semiempirical quantum mechanical calculations of the intercalation complexes were performed to predict charge transfer interactions of the carbazole chromophore of compounds **3**–**5** with selected DNA dinucleotides [19, 27]. The overall results of these investigations should be useful for a more rational antitumour drug design in the carbazole series.

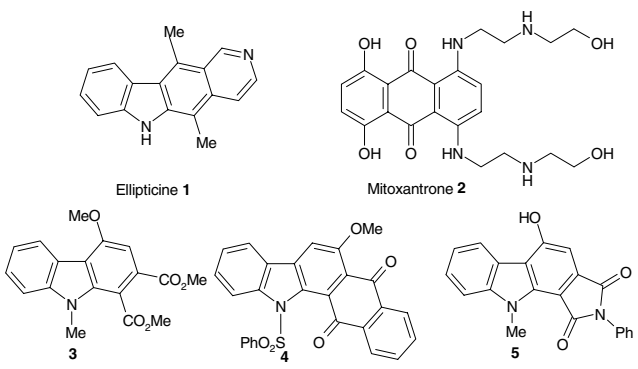

2. Investigations and results

2.1. DNA binding and tumour cell cytotoxicity

For a rational drug design of DNA binding drugs several methods of binding studies are described in the literature [28–30]. Among these methods, the ethidium bromide displacement assay has been established as a valuable preliminary tool for the determination of the extent of binding of a drug to DNA [20, 22, 23, 31, 32]. Moreover, as an indication of the intercalation process of a DNA ligand, the topoisomerase I unwinding assay has been confirmed as a reliable procedure [7, 24, 25]. These two methods were used experimentally to analyse the binding of the carbazoles **3**–**5** towards B-DNA. For the evaluation of the tumour cell cytotoxicity of these compounds the microtiterplate tetrazolium assay (MTT assay) was used [17].

2.1.1. Ethidium bromide displacement assay

The DNA binding affinity of the compounds **3**–**5** was assessed using the ethidium bromide displacement assay based upon a fluorimetric titration [31–33]. The intercalation of ethidium bromide in the DNA results in the formation of a fluorescent complex, the fluorescence intensity of which is reduced by adding a DNA binding drug since this displaces ethidium bromide from the DNA itself. The concentration of a drug leading to 50% reduction in the fluorescence intensity of the ethidium-DNA complex is defined in the literature as the C_{50} value [31–33]. This value represents the drug concentration necessary to displace 50% of the DNA bound ethidium. The C_{50} value is inversely proportional to the apparent binding constant value of the drugs but does not necessarily directly give a real binding constant because the mode and stoichiometry of binding of ethidium, an aromatic intercalator, and the studied drugs would probably be different [32, 33]. However, this assay leads to reliable results for qualitative comparisons of DNA binding abilities of a series of related compounds. The drugs Hoechst 33258 as a minor groove binder, ellipticine and mitoxantrone as intercalators and amsacrine as an intercalator with a groove binding side chain were used as reference compounds [6, 19, 34,

35]. Their C_{50} values are summarised in Table 1: a lowering of the concentration leading to 50% of the initial fluorescence indicates an increased DNA affinity (a greater K_a value) [21, 34, 36].
However the reduction to 50% fluorescence could not be achieved experimentally with any of the analysed substances **3**–**5** because of solubility problems (Table 1; Fig. 1). Compounds **3** and **5** gave a decrease in fluorescence, which was comparable to that due to the solvent (dilution effect). Compound **4** gave an evaluable but smaller decrease in fluorescence intensity than the reference substances, indicating a relatively low affinity.

Table 1: C_{50} values and binding constants [$\times 10^{-6}$ M and $\times 10^{6}$ M^{-1}, respectively] of compounds 3–5 and of reference substances [21, 34, 36]

Compd.	C_{50}	Lit-K_a	Calculated K_a
Hoechst 33258	8.38 ± 0.58	7	2.68 ± 0.17
Ellipticine	9.87 ± 1.90	0.85	2.28 ± 0.37
Mitoxantrone	0.45 ± 0.05	40	50 ± 5
Amsacrine	27.41 ± 1.87	0.14	0.82 ± 0.05
3	–	–	–
4	131.5 ± 4.5*	–	0.17 ± 0.01
5	–	–	–

* extrapolated

2.1.2. Unwinding assay

Unwinding of the double strand of the DNA helix is a hallmark feature of intercalating drugs such as ellipticine or mitoxantrone. For characterisation of novel compounds it is important to determine their eventual ability to intercalate. The topoisomerase I-unwinding assay allows the analysis of the effect of a compound on the distribution of DNA topoisomers generated by relaxation of closed circular DNA (supercoiled, form I) with topoisomerase I [37–39]. After incubation with topoisomerase I, the DNA is fully relaxed (form IV) which means that the linking number (Lk) is the twisting number (Tw) and the writhing number (Wr) is zero [38, 39]. Upon intercalation by a drug or reagent Tw is reduced but in the presence of topoisomerase, the equilibrium distribution of topoisomers is adjusted by the enzyme itself. Upon terminating the reaction and extracting the DNA so that protein and drug are removed, the DNA shrinks. This can be revealed by agarose gel electrophoresis (Fig. 2). One important caveat is to be sure that the test drug is not inhibiting the topoisomerase I activity which is essential for the assay. Comparison of the DNA unwinding with well known intercalators such as ellipticine and mitoxantrone and with groove binders such as Hoechst 33258 gives some idea of the potency of DNA binding of the three tested compounds. After incubation with topoisomerase I and DNA extraction, Wr is still zero and Lk is Tw: the DNA is in form IV (Fig. 2), thus the compounds are not intercalating agents or they are inhibiting the topoisomerase I.

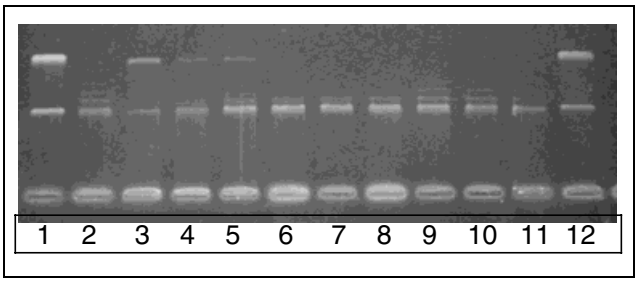

Fig. 2: Agarose gel electrophoretogram; lines 1 and 12: supercoiled DNA (Form I); line 2: DNA after incubation with topoisomerase I (relaxed, form IV); lines 3, 4, 5: 100 μM ellipticine, mitoxantrone and Hoechst 33258, respectively; lines 6 and 7: compound **3**, 10 and 100 μM respectively; lines 8 and 9: compound **4**, 10 and 100 μM respectively; lines 10 and 11: compound **5**, 10 and 100 μM respectively

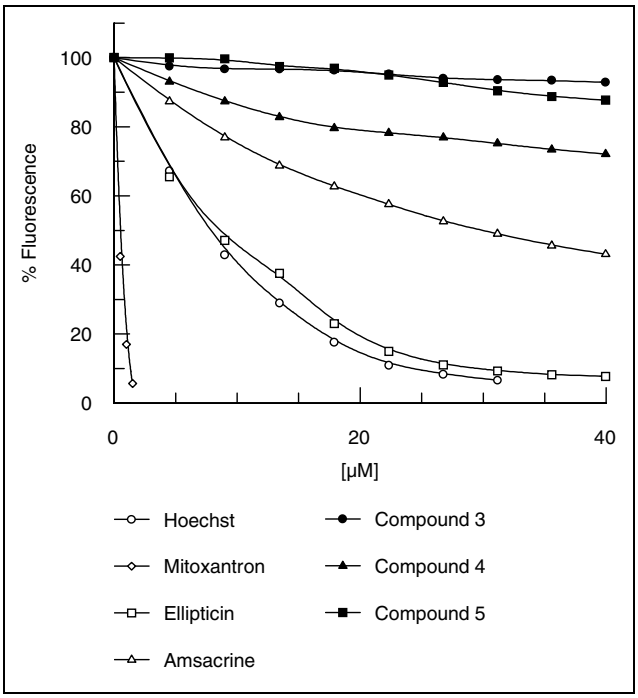

Fig. 1: Ethidium bromide displacement assay: reference compounds and carbazoles **3**–**5**. Compound **4** shows a slight, but clearly evaluable fluorescence quenching

2.1.3. Topoisomerase I inhibition assay

Topoisomerase I introduces into DNA at specific sites transient nicks, which lead to relaxation of the DNA helix. Incubation of the DNA-topoisomerase I mixture in the absence or presence of an active drug results in different population distributions of DNA topoisomers which can be revealed by gel electrophoresis. Comparison of the obtained plasmid DNA forms (supercoiled or relaxed) will indicate the ability of the tested drug to inhibit the enzyme. After incubation of plasmid DNA with topoisomerase I in the presence of compounds **3**–**5**, the DNA appeared in the supercoiled form (form I). This result reveals that the three compounds are inhibiting the topoisomerase I (Fig. 3).

2.1.4. Cytotoxicity assay

The relative cytotoxicity of compounds **3** and **4** towards four different human tumour cell lines was evaluated using the *in vitro* MTT assay as a primary screening method [17, 18]. Compound **4** shows a significant cell growth inhibition towards three tested cell lines (Table 2). Referring to the highly active anthracycline antibiotic doxorubicin (IC_{50} 0.037 mmol, L1210 cell line) or to ellipticine **1** (IC_{50} 0.99 mmol, L1210 cell line) both compounds **3** and **4** are weakly active [17, 18].

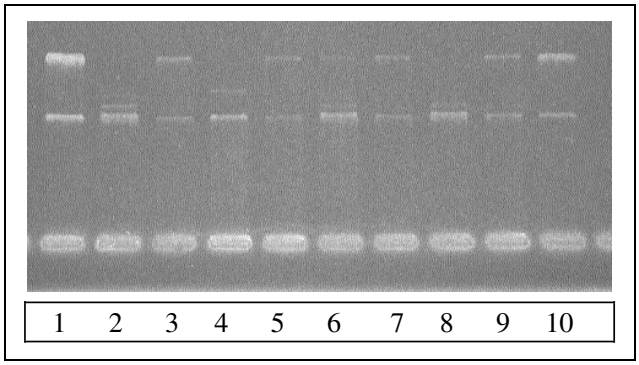

Fig. 3: Agarose gel electrophoretogram; lines 1 and 10: supercoiled DNA (form I); line 2: relaxed DNA (form IV); line 3: 100 μM camptothecin; lines 4 and 5: compound **3**, 10 and 100 μM respectively; lines 6 and 7: compound **4**, 10 and 100 μM respectively; lines 8 and 9: compound **5**, 10 and 100 μM respectively

2.2. Molecular modeling studies

The application of molecular modeling techniques in nucleic acid chemistry can effectively rationalize ligand DNA interactions at the atomic level [46, 58, 59]. Thus, the theoretical information about binding characteristics, molecular connections at the atomic level and energetic aspects including information of DNA base selectivity can be very helpful to support structure activity relationships. Moreover, this technique can be useful for the design and structural optimization of new biologically active DNA ligands. In continuation of our DNA ligand molecular modeling studies we have constructed and minimised carbazole DNA complexes employing molecular mechanics, molecular dynamics and semiempirical (MO-) methods [7, 26, 27, 35, 40]. The obtained results should rationalize and complete the experimental findings of chapter 2.1. Distinct details about the molecular modeling procedure are reported elsewhere [19].

2.2.1. Minimisation of the ligands

The crystal structures of the carbazoles **3**–**5** were minimised by semiempirical quantum mechanical methods (see 4.4) to get the necessary ESP-charges of the carbazoles and were taken as starting geometries for the following calculations [16, 17, 41, 52]. The carbazole nitrogen of compound **4** is set to planar in the molecular mechanics and molecular dynamics calculations, although it is slightly pyramidal in the crystal structure (Σ 342.8°) [42]. While minimising **4** with the TRIPOS force field, this leads to much better RMS values of 0.06 (0.42) vs. 0.09 (0.72) Å · kcal · mol^{-1}, concerning the aromatic system without hydrogens (in parentheses: all non-hydrogens; SYBYL option RMS_DEVIATION) [42]. This procedure was applied to validate the molecular mechanics calculations.

Table 2: IC_{50} (growth inhibitory concentration, [mmol]) and LC_{50} (lethal concentration, [mmol]) of the carbazoles 3 and 4 [17]

Cell line[a]	carbazole 3		carbazole 4	
	IC_{50}	LC_{50}	IC_{50}	LC_{50}
K562 (chronic myeloid leukaemia)	200	–	25	–
RXF393 (kidney tumour)	100	190	30	85
HCT116 (colon cancer)	>100	>100	>100	>100
SKmel28 (malignant melanoma)	>100	>100	50	60–78

[a] MTT – cytotoxicity assay, primary screening method performed at the National Cancer Institute, Frederick Cancer Research and Development Centers, Frederick, MD (USA)

2.2.2. Generation of carbazole/DNA-complexes

As planar aromatic compounds carbazoles and anellated derivatives should principally be able to intercalate between the DNA base pairs [1, 14, 50]. In order to receive molecular information about relevant conformation families and about the energetically favoured ligand/DNA intercalation complexes a suitable version of the molecular dynamics method published earlier by us was used [19, chapter 5.5]; for abbreviations see [43]. For the calculations B-DNA oligonucleotides with enlarged intercalation cavities between base pair 3 and base pair 4 were chosen [19]. The relevant building-up process was described in detail earlier [19]. After molecular mechanics refinement calculations, energetically favoured intercalation complexes of the carbazoles **3**–**5** with the DNA oligomers were obtained.

The intercalation complex of compound **3** into the cavity of dCG**TA**CG or by analogy into dCG**GC**CG is of special interest. It is shown in Fig. 4, left side. In this context the program GRID can be used to calculate interaction fields between a biopolymer target (the DNA) and a partial structure (e.g. the aromatic system with an aromatic "probe") of the respective ligand [19, 44]. These calculations may also be useful for the construction of reasonable starting geometries for docking procedures and molecular dynamics simulations. Fig. 4, right side, visualises the interaction patterns as isoenergy contour fields, which show clearly that a favoured intercalation of the aromatic system is characterised a) by an edge – on alignment orientation,

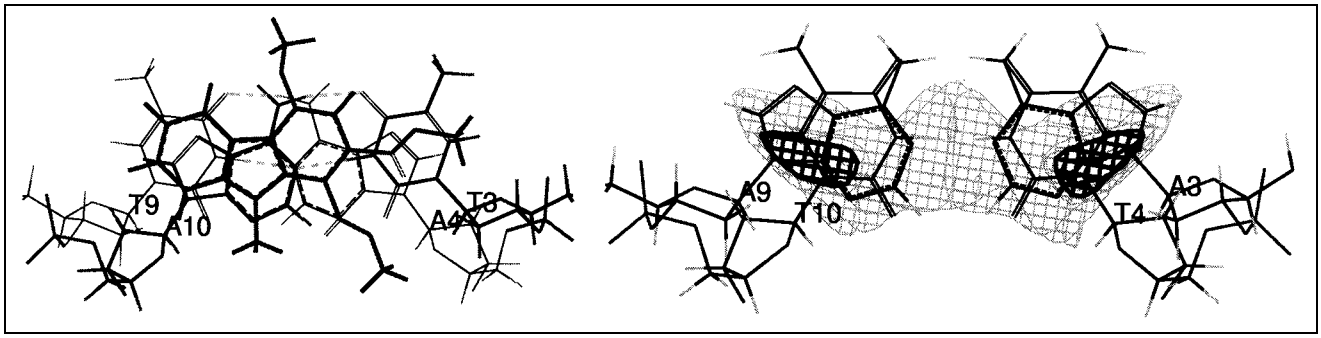

Fig. 4: Left side: Intercalation complex of compound **3** in the dTA cavity of the base paired DNA hexamer dCG**TA**CG, top view. Only cavity and ligand (in bold) are shown. The base pair and the carbazole **3** are parallel to the plane of view. The base pair A10–T3 is above and the base pair A4–T9 is below the intercalation in this projection of the cavity. One side chain intercalates, the other one penetrates into the minor groove. For abbreviations see [43]; for details of the application see [19]. Right side: Interaction fields calculated for an aromatic probe in a dAT cavity [44]. A maximum energy gain by intercalation of an aromatic compound is possible by an edge – on alignment of the aromate combined with a shift towards one DNA strand as found for compound **3**, left side. Isoenergy contour field coding: bold lines −4.2, grey lines −3.0 kcal · mol^{-1}

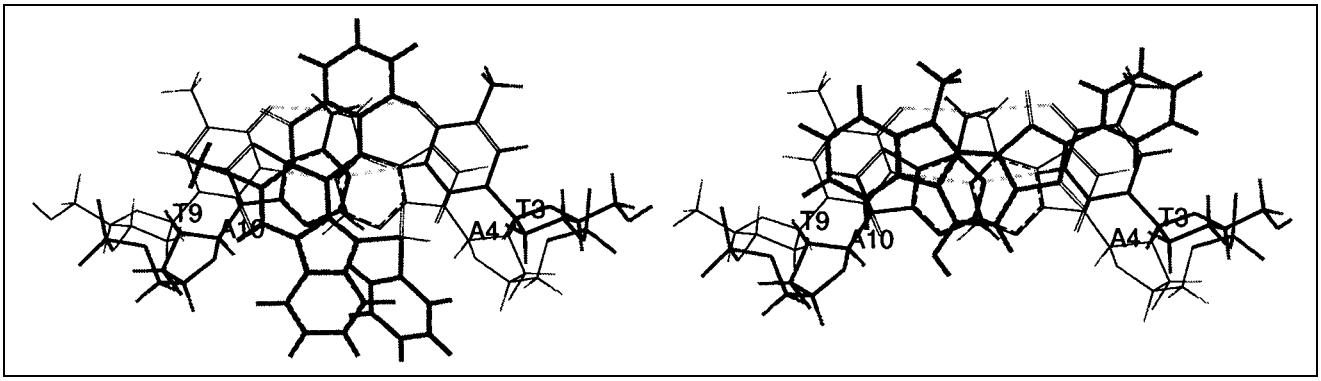

Fig. 5: Left side: Intercalation complex of compound **4** in the dTA cavity of the DNA hexamer dCG**TA**CG. Only cavity and ligand (in bold) are shown. Again the top view of the intercalation complex is shown, see text of Fig. 4. Right side: Intercalation complex of compound **5** in the dTA cavity of dCG**TA**CG, top view. The pyrrolocarbazole **5** is intercalated in an edge – on alignment orientation as compound **3**, see Fig. 4 [45]

and b) by the shift of the ligand inside the cavity to one strand of the DNA. This simulated ligand orientation can be found exactly for the energetically favoured intercalation complexes of compound **3** by molecular dynamics calculations as shown in Fig. 3.

Moreover, on the basis of the molecular dynamics and mechanics calculations compound **4** favours an intercalation perpendicular to the cavity of the DNA hexamers dCG**TA**CG and dCG**GC**CG probably due to the steric hindrance of the bulky *N*-phenylsulfonyl group, as shown in Fig. 5, left side. The side chain of the ligand exhibits good van der Waals contacts in the minor groove. This minor groove interaction is also found for amsacrine derivatives [19].

The planar, V-shaped pyrrolocarbazole **5** intercalates almost totally in an edge – on alignment mode into the cavity of dCG**TA**CG or dCG**GC**CG. The phenyl ring is partially intercalated, pointing towards the major groove side, see Fig. 5. The hydroxy group is located in the minor groove, often forming hydrogen bonds especially to the acceptor atoms of the bases.

Fig. 6 presents a summary of the force field energy partial terms of the favoured intercalation complexes. It is obvious that all candidates **3**–**5** favour the dGC cavity of the DNA hexamer dCG**GC**CG. G/C cavities are considered to be similar or energetically favoured compared to A/T cavities in these series of structurally related compounds [27, 45, 46]. Each of the compounds **3**–**5** reflects a high energy gain [$\Delta E_{netgain}$] because of favourable van der Waals contacts [ΔE_{vdW}]. The other partial terms are small because the ligands are not charged (resolution in a low ΔE_{El}) and sterically modest (low ΔE_R and ΔE_{BAT}).

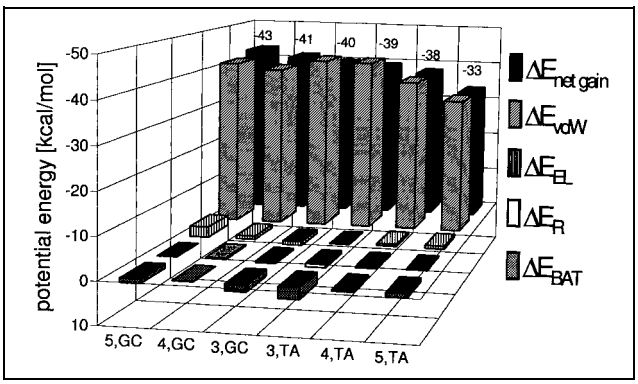

Fig. 6: A survey of the potential force field energy and the partial terms (kcal · mol^{-1}) of the intercalation complexes of the carbazole derivatives **3**–**5**. The DNA hexamers dCG**TA**CG (= TA) and dCG**GC**CG (= GC) were fixed during the calculations. The side chain of **4** is orientated in the minor groove. For further details of the protocol see ref. [19]. Stabilising energy contributions yield negative values (upward columns), destabilising contributes to the total energy yield positive values (downward columns)

The energies are calculated according to the TRIPOS force field implemented in the SYBYL program package [27, 42]:

$$\Delta E_{\text{net gain}} = \Delta E_{vdW} + \Delta E_{El} + \Delta E_R + \Delta E_{BAT}\ [\text{kcal} \cdot \text{mol}^{-1}]$$

$$\Delta E_{vdW} = \Delta E_{\text{van der Waals interactions}} = E_{\text{vdW complex}} - E_{\text{vdW DNA}} - E_{\text{vdW ligand}}\ ;$$

$$\Delta E_{El} = \Delta E_{\text{electrostatic interactions}} = E_{\text{El complex}} - E_{\text{El DNA}} - E_{\text{El ligand}}\ ;$$

$$\Delta E_R = E_{\text{R complex}} - E_{\text{R DNA}} - E_{\text{R ligand}}\ ;$$

$$E_R = E_{\text{out of plane-bending}} + E_{\text{1–4 van der Waals interactions}} + E_{\text{1–4 electrostatic interactions}}\ ;$$

$$\Delta E_{BAT} = E_{\text{BAT complex}} - E_{\text{BAT DNA}} - E_{\text{BAT ligand}}\ ;$$

$$E_{BAT} = E_{\text{conformational energies}} = E_{\text{bond stretching}} + E_{\text{angle bending}} + E_{\text{torsional}}\ .$$

2.2.3. Prediction of charge transfer (CT) interactions

Charge transfer interactions represent another contribution to the stability of intercalation complexes [19, 27, 39, 55]. In order to predict this interaction of a drug with the respective target, semiempirical MO calculations represent a reliable method for analysing the relevant frontier orbitals involved in an orbital overlapping between the electron deficient chromophore and the respective DNA bases [27, 41, 46]. Our earlier reported calculations revealed that a charge transfer interaction will be electronically favoured if the chromophoric system of the intercalator exhibits pronounced electron deficiency [19, 27, 42]. According to the frontier molecular orbital model the quinoid compound **4** reveals CT interactions although it is intercalated perpendicularly. This orientation geometry enables only a partial orbital overlap of the DNA bases and the ligand (Fig. 5). The localisations of HOMO and LUMO are in different subsystems. An appropriate difference of 7.3 eV ($\Delta H_f\ HOMO_{dTA} - \Delta H_f\ LUMO_{ligand}$) and 6.4 eV ($\Delta H_f\ HOMO_{dGC} - \Delta H_f\ LUMO_{ligand}$) between the frontier molecular orbitals can be found, and the magnitude and sign of the p_z – coefficients of the orbitals fit CT conditions [19, 27, 48, 49]. The carbazoles **3** and **5** show a good overlap with the DNA – bases (Figs. 4 and 5), but no CT – interactions can be postulated. The HOMOs of both complexes are mainly located in one adenine base, but other substructures share unfavourably HOMO and LUMO frontier orbitals, sometimes showing additionally high p_z – coefficients in the orbitals [27, 48, 49].

Table 3: Method I: Molecular dynamics simulation cycles [19, 54]

Cycle no.	Length of interval (fs)	Step (fs)	Snap-shot (fs)	Temp.-coupling (K)	Temp.-tolerance (fs)	Non-bonded contacts (Å)	Update (fs)
1	600	1	600	500	10	0.0001	1
2/4/6/8/10	2000	1	500	50	10	0.0001	1
3/5/7/9	300	1	300	500	10	0.0001	1

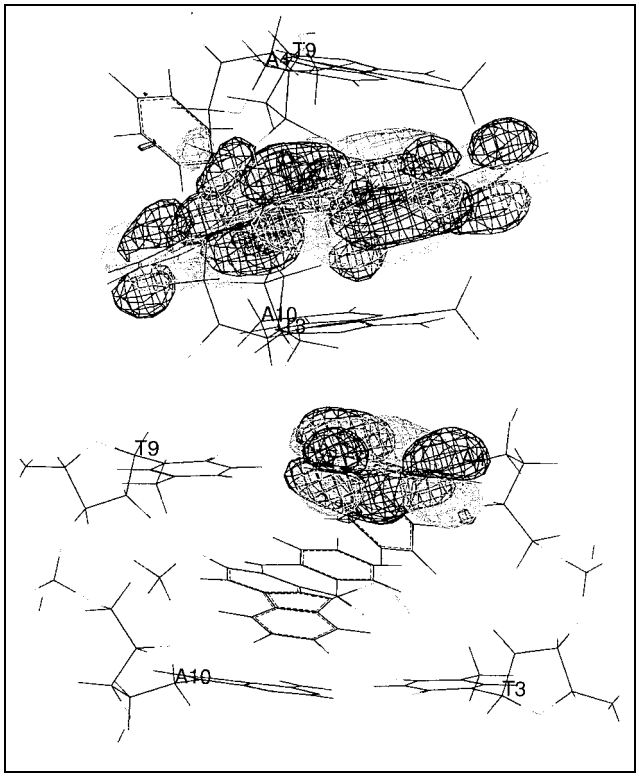

Fig. 7: Frontier molecular orbital derived CT interactions of the intercalation complex of the carbazole **4** in dCG**TA**CG (see Fig. 4), calculated for the dTA cavity plus ligand as shown [40, 41]. Upper part: The LUMO is mainly located in the naphthoquinone unit of the ligand. Lower part: The HOMO of the same complex is shown. The HOMO is nearly totally located in one adenine base

3. Discussion

The *in vitro* experimental findings revealed that the quinoid carbazole **4** exhibits sufficient tumour cell cytotoxicity towards the cell lines K562 and RXF393 of this series (Table 2). Moreover, the DNA binding studies reflect a weak, but analytically reliable, binding affinity for this compound (Table 1). These preliminary results suppose that DNA is the primary target for the biological effects. Moreover, the theoretical results also predict the interaction of **4** with DNA oligonucleotides. Thus the data which we have obtained from the molecular modeling studies should describe the reality from a theoretical point of view. In this context charge transfer interactions can be postulated only for the energetically favoured intercalation complexes of compound **4** in a dGC cavity or in a dTA cavity. This fits the fact that compound **4** shows a higher in vitro activity in the MTT test if compared with compound **3** and that carbazole **4** shows an analytically evaluable fluorescence reduction in the ethidium bromide assay. Looking at dCG**GC**CG intercalation complexes the energy gains calculated by using the TRIPOS force field show also the ranking found by the MTT test: compound **4** possesses a higher activity than **3**. The difference between the energy gain found for compounds **3** and **4** intercalated into dCG**TA**CG 1.4 kcal · mol^{-1} is very small. The TRIPOS force field is not able to calculate charge transfer interactions, though they lead to equally high stabilising energy gains as are found for strong hydrogen bonds [44, 45, 50, 55, 56]. If they were taken into consideration, compound **4** intercalated into dCGGCCG would have a much higher energy gain than **3** and would thus also fit the experimental data. However, the ability to intercalate into DNA could not be determined with the unwinding assay because the compounds showed an inhibition of the topoisomerase I which is necessary for succeeding this test. This unexpected activity could explain the better cytotoxicity of compound **4**, compared to the other compounds. In any case, in the present group of compounds carbazole **4** should be the most promising lead compound for a further structural variation in the design of new antitumour active drugs in the carbazole series.

To determine the intercalation potency of each of the three lead compounds **3**–**5** additional tests should be made, which do not require topoisomerase I as a reagent. Chemical efforts will be made to modify the compounds for better solubility and higher binding constants. In particular, the addition of hydrophilic side chains (e. g. with protonable amino groups similar to mitoxantrone, **1**) may be an important feature for further synthetic studies in carbazole drug design [26, 27, 57].

4. Experimental

4.1. Ethidium bromide displacement assay

All fluorescence measurements were conducted on an Hitachi F-2000 spectrofluorometer. Calf thymus DNA (Sigma, Type I; 1.0×10^{-5} M in base pairs) was added in small aliquots to ethidium bromide (GIBCO BRL; 5.0×10^{-6} M) resulting in a 2 : 1 ratio of base pair/ethidium bromide in 2 ml of a 10 mM Tris-HCl (pH 7.4), 75 mM NaCl buffer solution [20, 22]. The fluorescence of the DNA-ethidium buffer solution was calibrated at room temperature to 100% F and that of the ethidium buffer solution to 0% F, respectively. The premixed DNA-ethidium solution was titrated with 3 µl aliquots of the stock solution of the test substances (3 mM drug in DMSO) and stirred at room temperature for 30 min prior to each fluorescence measurement. The fluorescence was measured with 545 nm excitation and 595 nm emission with a slit width of 10 nm. The binding affinity was determined at 50% ethidium bromide displacement, measured as a drop in fluorescence to 50%. Results were calculated with the Data Analysis and Graphics Program GRAFIT (Table 1, Fig. 1). Apparent binding constants (K_a) were calculated from the C_{50} values using: $K_a = K_{EtdBr}[EtdBr]/C_{50}$ and with a value of $K_{EtdBr} = [4.5 \times 10^{-6}]$ for ethidium bromide [22, 32]. Hoechst 33258 (Acros), ellipticine (Fluka) and amsacrine (Gödecke) as reference compounds were tested in the same way.

4.2. Unwinding assay

Plasmid DNA (pUC 19, GIBCO; 0.033 µg/µl) was incubated for 30 min at 37 °C with topoisomerase I (GIBCO; 0.16 U/µl) in topoisomerase I reaction buffer (50 mM Tris HCl pH 7.5, 50 mM KCl, 10 mM MgCl, 0.5 mM DTT, 0.1 mM EDTA, 30 µg/ml BSA). The mixture containing relaxed plasmid DNA was given in 10 µl aliquots to the solutions of different concentrations of the drugs (10 and 100 µM). After 1 h at 37 °C, the reaction mixtures were treated with TE-Buffer (pH 7.9) and extracted twice with Phenol/CIA solution (chloroform : isoamylalcohol 24 : 1) 1 : 1 and once with CIA-solution. Sodium acetate and absolute ethanol were added to the upper solution which was then incubated for 1 h at −20 °C and spun briefly in a microfuge. The DNA pellet was then dried, dissolved in 20 µl loading dye and loaded onto a 1% agarose gel (Tris-Glycine-Buffer) which was run for 4 h at 55 V.

4.3. Topoisomerase I inhibition assay

Plasmid DNA (pUC 19, GIBCO; 0.033 µg/µl) was incubated for 30 min at 37 °C with topoisomerase I (GIBCO; 0.16 U/µl) in 1× topoisomerase I Reaction Buffer (50 mM Tris HCl pH 7.5, 50 mM KCl, 10 mM MgCl,

0.5 mM DTT, 0.1 mM EDTA, 30 μg/ml BSA) in the presence of different concentrations of the tested drugs (10 μM and 100 μM). After extracting DNA by the same procedure as above, gel electrophoresis was run under the same conditions.

4.4. Energetical minimisation of the ligands

The crystal structure geometries of the compounds **3**–**5** were minimised with the semiempirical quantum chemical program MOPAC 6.0, key words XYZ AM1 MMOK (last refinement: PRECISE, ESP) [16, 17, 41, 52]. Force fields minimization of **4** for validation purposes: default values were used except for POWELL conjugate gradient minimizer, RMS – GRADIENT break – off criteria Δ 0.01 kcal $\cdot$ mol^{-1} $\cdot$ Å^{-1}, max. 500 iterations and MOPAC/AM1 charges [41, 42].

4.5. Generation of carbazole/DNA-complexes

For the molecular mechanics and molecular dynamics calculations the respective tools in the program package SYBYL 6.02 were used [42]. DNA hexamers: Gasteiger Hückel charges, no counterions; each phosphate group has a charge of −1; the DNA was fixed as aggregate [42, 51]. This procedure has been approved in related molecular modeling studies of DNA complexes [26, 27, 46, 51]. Ligands: the MOPAC/AM1 minimised structures (chapter 4.4.) were used and assorted with MOPAC 6.0 AM1/ESP charges [41, 52].

4.5.1. Molecular dynamics simulations (MD)

The base paired DNA hexamers dCG**TA**CG and dCG**GC**CG with the enlarged cavity of 6.8 Å between the base pairs 3 and 4 had been interactively constructed using appropriate crystal structures and were minimised by molecular mechanics [19, 42, 43, 46]; for details see ref. [19]. As starting geometry the intercalator was interactively docked into the DNA cavity using the SYBYL option DOCK and was minimised according to method II (chapter 4.5.2.) [42]. Starting from four up to seven constructed intercalation complexes the MD calculations were run using SYBYL 6.02, see Table 3. The DNA was fixed as aggregate. Parameters used: dielectric constant = 4.0, distance dependent function; non bonded cut off 20.0 Å; NTV – ensemble: N = constant number of n atoms in the ensemble, T = constant, V = constant volume; kinetic energy scaled after each time interval at the given temperature [42, 46, 53].

4.5.2. Minimisation of the complexes (molecular mechanics calculations)

Method II: SYBYL 6.02, POWELL conjugate gradient minimiser [42, 48]; RMS – GRADIENT break off criteria Δ 0.01 kcal $\cdot$ mol^{-1} $\cdot$ Å^{-1}, max. 1000 iterations. Non bonded contacts: 8.0 Å, dielectric constant e = 4.0, distance dependent function [19, 39, 44].

4.6. Calculation of frontier orbitals for prediction of charge transfer interactions

The molecular orbital (MO) calculations for analysing charge transfer (CT) interactions of the intercalated ligand together with the surrounding dinucleotide were performed with MOPAC 6.0/AM1 [41]. The negative partial charges of the phosphate groups were neutralised by adding hydrogens, even so to the 5′- and 3′-oxygens of the cut off dinucleotides revealing hydroxy groups. MOPAC key words: VECT AM1 1SCF MMOK. For visualisation see [47].

4.7. Hardware

The program package SYBYL 6.02 was installed on VAX 4000/90 and 4000/60 machines, SYBYL 6.31 on a SGI-High Impact machine, the MOPAC calculations were performed on ALPHA calculation machines DEC 3000 M300, DEC 2100 A500 MP or DEC 8400 5/300 of the Zentrum für Datenverarbeitung, Universität Mainz. A TRANSDEC TT401 (DEC VT220) and an IBM RISC RS 6000 computer as X-terminal were used.

Acknowledgements: We thank the Deutsche Forschungsgemeinschaft, Bonn, for financial support and the Gödeke Industry for the compound amsacrine.

References

1 Gribble, G. W.; in: Brossi, A. (ed.): The Alkaloids, Vol. 39, p. 239, Academic Press, New York, London, 1990
2 Chakraborty, D. P.; Roy, S.; in: Herz, W.; Krby, G. W.; Steglich, W.; Tamm, C. (eds.): Fortschr. Chem. Org. Naturst.; Vol. 57, p. 71, 1991
3 Bergman, I.; in: Atta-ur-Rhaman (ed.): Studies in Natural Products Chemistry, Vol. 1, p. 8, Elsevier, Amsterdam 1988
4 Kuckländer, U.; Pitzler, H.; Kuna, K.: Arch. Pharm. **327**, 137 (1994)
5 Segall, A.; Pappa, H.; Causabon, R.; Martin, G.; Bergoc, R.; Pizzorno, M. T.; Eur. J. Med. Chem. **30**, 165 (1995)
6 Pindur, U.; Haber, M.; Sattler, K.; J. Chem. Educ. **4**, 263 (1993)
7 Sattler, K.; Thesis, University of Mainz 1994
8 Pierre, A.; Atassi, G.; Devissaguet, M.; Bisagni, E.: Drugs Fut. **22**, 53 (1997)
9 Juret, P.; Tanguy, A., Girard, A.; Le Pecq, J.-B.; Paoletti, C.; Eur. J. Cancer **14**, 205 (1978)
10 Panousis, C.; Phillips, D. R.; Nucleic. Acids Res. **22**, 1342(1994)
11 Mazerski, J.; Martelli S.; Borowski E.; Acta Biochim. Pol. **45**, 1 (1998)
12 Babaian, I. S.; Manzini, G.: Mol. Biol. Mosk. **24**, 1084 (1990)
13 Gonzales, E.; Pindur, U.; Schollmeyer, D.: J. Chem. Soc., Perkin Trans. I, 1767 (1996)
14 Pindur, U.; in: Moody, C. J. (ed.): Adv. in Nitrogen Heterocycles, Vol. 1. p. 121, JAI Press, Greenwich 1995
15 Pindur, U.; Lemster, T.: Transworld Res. Network **1**, 33 (1997)
16 Schollmeyer, D.; Fischer, G.; Pindur, U.: Acta Cryst. **C 52**, 1277 (1996)
17 Rogge, M.; Fischer, G.; Schollmeyer, D.; Pindur, U.: Monatsh. Chem. **127**, 97 (1996)
18 Weinkauf, R. L.; La Voie, E. J.: Bioorg. Med. Chem. **2**, 781 (1994)
19 Fischer, G.; Pindur, U.: Pharmazie **54**, 83 (1999)
20 Morgan, A. R.; Lee, J. S.; Pulleyblank, D. E.; Murray, N. L.: Nucleic Acids Res. **7**, 547 (1979)
21 Wilson, W.; Baguley, B. C.; Wakelin, L. P. G.; Waring, M. J.: Mol. Pharmacol. **20**, 404 (1981)
22 Boger, D. L.; Chen, J-H.; Saionz, K. W.: J. Am. Chem. Soc. **118**, 7 (1996)
23 Antonini, I.; Polucci, P.; Jenkins, T. C.; Kelland, L. R.; Menta, E.; Pescalli, N.; Stefanska, B.; Mazerski, J.; Martelli, S.: J. Med. Chem. **40**, 3749 (1997)
24 Kim, J. S.; Sun, Q.; Gatto, B.; Yu, C.; Liu, A.; Liu, L. F.; La Voie, E. J.: Bioorg. & Med. Chem. **4**, 621 (1996)
25 Bonnard, I.; Bontemos, N.; Lahmy, S.; Banaigs, B.; Combaut, G.; Francisco, C.; Colson, P.; Houssier, C.; Waring, M. J.; Bailly, C.: Anti-Cancer Drug Des. **10**, 333 (1995)
26 Rehn, C.; Pindur, U.: Monatsh. Chem. **127**, 631 (1996)
27 Rehn, C.; Pindur, U.: Monatsh. Chem. **127**, 645 (1996)
28 Suh, D.; Chaires, J. B.: Bioorg. Med. Chem. **3**, 723 (1995)
29 Long, E. C.: Acc. Chem. Res. **23**, 271 (1990)
30 Fox, K. R.: Meth. in Mol. Biol., 90 (1997)
31 Hsieh, H-P.; Muller, J. G.; Burrows, C. J.: Bioorg. & Med. Chem. **3**, 823 (1995)
32 Wellmann, S. E.: Biopolymers **39**, 491 (1996)
33 Takenaka, J.; Sato, H.; Ihara, T.; Takagi, M.: J. Heterocycl. Chem. **34**, 123 (1997)
34 Frau, S; Bernardou, J.; Meunier B.: Bull. Soc. Chim. Fr. **133**, 1053 (1996)
35 Pindur, U.; Fischer, G.: Curr. Med. Chem. **3**, 325 (1996)
36 Dodin, G.; Schwaller, M.-A.; Aubard, J.; Paoletti, C.: Eur. J. Bioch. **176**, 371 (1988)
37 Pindur, U.; Lemster, T.: Pharmazie **53**, 79 (1998)
38 Voet, J.; Voet, J. G.; in: Biochemie, VCH Verlag, Weinheim 1994
39 Saenger, W.; in: Principles of Nucleic Acid Structure, Springer-Verlag/ Springer Advanced Texts in Chemistry, New York 1983
40 Rehn, C.: Thesis, University of Mainz 1995
41 MOPAC 6.0, QCPE 455; Steward, J. J. P.: J. Comput. – Aided Mol. Des. **4**, 1 (1990)
42 SYBYL 6.02, Tripos Assoc. Inc., St. Louis, USA 1993
43 Abbreviations used: e.g. dCGCGCG = DNA hexamer d(CpGpCpGpCpG)$_2$, A/T = A*T or T*A; BP = base pair; A = Ade, T = Thy, C = Cyt, G Gua
44 GRID, Vers. 9.02, Molecular Discovery Ltd, England, Oxford 1991
45 Chen, K.-X.; Gresh, N.; Pullman, B.: Nucleic Acids Res. **16**, 3061 (1988)
46 Neidle, S.; in: Beddell, C. R. (Ed.): The design of drugs to macromolecular targets, p. 173, J. Wiley & Sons Ltd., New York 1992
47 SYBYL 6.31, Tripos Assoc. Inc., St. Louis, USA 1996
48 Höltje, H.–D.; Jendretzki, U. K.: Arch. Pharm. **328**, 577 (1995)
49 Kunz, R. W.; in: Elschenbroich, C.; Hensel, F.; Hopf, H. (Eds.): Molecular Modeling für Anwender: Anwendung von Kraftfeld- und MO-Methoden in der organischen Chemie, Teubner, Stuttgart 1991
50 Jain, S. C.; Bhandary, K. K.; Sobell, H. M.: J. Mol. Biol. **135**, 813 1979
51 Rodger, A.; Taylor, S.; Adlam, G.; Blagbrough, I. S.; Haworth, I. S.: Bioorg. Med. Chem. **3**, 861 (1995)
52 Besler, B.; Merz, K. M.; Kollman, P. A.: J. Comp. Chem. **4**, 431 (1990)
53 Furet, P.; Caravatti, G.; Lydon, N.; Priestle, J. P.; Sowadski, J. M.; Trinks, U.; Traxler, P.: J. Comput.-Aided Mol. Des. **9**, 465 (1995)
54 Fantucci, P.; Marino, T.; Russo, N.; Villa, A. M.: J. Comput.-Aided Mol. Des. **9**, 425 (1995)
55 Mayoh, B.; Prout, C. K.: J. Chem. Soc., Perkin Trans. II, 1072 (1972)
56 Testa, B.: Grundlagen der Organischen Stereochemie (Übers.: Kübel, B.), Verlag Chemie Weinheim 1983
57 Fischer, G.: Thesis, University of Mainz 1997
58 Höltje, H. D.; Folkers, G.; in: Mannhold, R.; Kubinyi, H.; Timmermann, H. (Eds.): Molecular Modeling – Basic Principles and Applications, Vol. 5, VCH Verlagsgesellschaft mbH, Weinheim 1996
59 McKenna, R.; Beveridge, J.; Jenkins, T. C.; Neidle, S.; Denny, W. A.: Mol. Pharmacol. **35**, 720 (1989)

Received October 22, 1999
Accepted January 27, 2000

Prof. Dr. U. Pindur
Institut für Pharmazie
Staudinger Weg 5
D-55099 Mainz
pindur@mail.uni-mainz.de